Available online at www.sciencedirect.com

ScienceDirect

Geochimica et Cosmochimica Acta 237 (2018) 205–222

Geochimica et Cosmochimica Acta

www.elsevier.com/locate/gca

Contrasting Mg isotopic compositions between Fe-Mn nodules and surrounding soils: Accumulation of light Mg isotopes by Mg-depleted clay minerals and Fe oxides

Ting Gao [a,b,c], Shan Ke [d], Shui-Jiong Wang [d], Fangbai Li [b], Chengshuai Liu [a,b,*], Jing Lei [e], Changzhong Liao [b], Fei Wu [a,c]

[a] State Key Laboratory of Environmental Geochemistry, Institute of Geochemistry, Chinese Academy of Sciences, Guiyang 550081, PR China
[b] Guangdong Key Laboratory of Integrated Agro-Environmental Pollution Control and Management, Guangdong Institute of Eco-Environmental Sciences & Technology, Guangzhou 510650, PR China
[c] University of Chinese Academy of Sciences, Beijing 100049, PR China
[d] State Key Laboratory of Geological Process and Mineral Resources, School of Earth Science and Resources, China University of Geosciences, Beijing 100083, PR China
[e] College of Agriculture, Guangxi University, Nanning 530005, PR China

Received 25 September 2017; accepted in revised form 22 June 2018; available online 30 June 2018

Abstract

Magnesium isotopic systematics has been increasingly used to trace the biogeochemical cycle of Mg in soil systems, and Fe oxides are the critical soil components that affect the geochemical behaviours of elements in soils. The role of Fe oxides in fractionating Mg isotopes, however, remains unclear. Here, Mg isotopic compositions are reported for typical Fe-Mn nodules (FMNs), surrounding soils, soil waters, and soil surface waters for a paddy soil profile, and stream waters, and rainwaters in southwestern China to improve our understanding of the processes that control the Mg isotopic compositions in soil systems. Further sequential extraction experiments are conducted to separate two pools of Mg in the FMNs and soils: structural Mg and exchange Mg. The FMNs (−1.39 to −1.58‰) are isotopically lighter than surrounding soils (−0.59 to −0.85‰) but heavier than soil waters (−1.59‰), and surrounding soils are isotopically lighter than parent granite (−0.25‰). The difference in Mg isotopic compositions between FMNs and surrounding soils reflects different sources of Mg in the mineral crystal structures. Structural Mg in surrounding soils is mainly from the chemical weathering of parent granite. By contrast, structural Mg in FMNs is from soil waters because of the frequently repeated dissolution and precipitation of Fe oxides under alternating redox conditions. Enrichment of heavy Mg isotopes in the FMNs relative to soil waters results from preferential incorporation of ^{26}Mg via Mg^{2+} substitution for Fe^{3+} in goethite. Given that the exchangeable Mg (−1.62 to −1.91‰) is significantly enriched in light Mg isotopes, the lighter Mg isotopic compositions in surrounding soils relative to their parent granite can be explained by the retention of light Mg isotopes in exchangeable sites of Mg-depleted minerals (kaolinite). Exchangeable Mg in FMNs (−1.79 to −2.15‰) is also shown to be enriched in light Mg isotopes. These light isotopic compositions of exchangeable Mg can be explained by a combination of carbonate contribution and isotope fractionation processes on the soil exchange fractions. Ion-exchange processes preferentially remove heavy Mg isotopes from soil minerals, leaving soil exchange fractions hosting light Mg isotopes. Additionally, river waters draining carbonates contributes light Mg isotopes to soil exchangeable fractions. Our study demonstrates that the development of Mg-depleted clay minerals and Fe oxides can

* Corresponding author at: State Key Laboratory of Environmental Geochemistry, Institute of Geochemistry, Chinese Academy of Sciences, Guiyang 550081, PR China.
E-mail address: liuchengshuai@vip.gyig.ac.cn (C. Liu).

https://doi.org/10.1016/j.gca.2018.06.028

considerably lower the soil δ^{26}Mg values, highlighting the major roles of these two soil minerals in controlling soil Mg isotopic compositions.

Keywords: Mg isotopes; Soils; Fe oxides; Mg-depleted clay mineral; Exchangeable Mg

1. INTRODUCTION

The biogeochemical cycle of Mg, which is a macronutrient in soil zone, is closely related to the growth of plants because Mg participates in chlorophyll synthesis and catalytic action (Montezano et al., 2013). Soils with low concentrations of Mg can decrease agricultural productivity and quality. It is therefore important to understand behaviours of Mg in soil systems, i.e., the distribution, mobility, and bioavailability of Mg in different reservoirs, including clay minerals, metal oxides, soil waters, and vegetation.

Magnesium has only one redox state (+2) and is thus insensitive to changes in oxygen fugacity (Teng, 2017). In soils, Mg^{2+} ions are mostly adsorbed at surfaces/interlayers ("exchangeable Mg") and incorporated into the crystal structures ("structural Mg") of clay minerals and Fe/Mn oxides (Kinniburgh et al., 1976; Odom, 1984; Drever, 1988; Merkel and Planer-Friedrich, 2008; Jolsterå et al., 2012; Montezano et al., 2013). Exchangeable Mg is relatively weakly bonded and can exchange with other metal ions. The adsorption of Mg^{2+} ions onto a variety of secondary minerals strongly depends on the surface charge properties of minerals, i.e., the pH of the point of zero charge (pH_{pzc}) (Scroth and Sposito, 1997; Kosmulski, 2006). In addition, Mg^{2+} ions can be complexed by organic matter (Montezano et al., 2013). The remaining Mg^{2+} ions are mostly dissolved in soil waters ("dissolved Mg") in the form of hydrated ions (Pavlov et al., 1998), which can exchange with other exchangeable metal ions or be taken up by vegetation (Wilkinson et al., 1990).

Magnesium isotope geochemistry potentially provides a powerful tool to trace the environmental behaviours of soil Mg because its isotopes are significantly fractionated by both biotic and abiotic processes at surface environments (Schmitt et al., 2012; Teng, 2017). The fractionation of Mg isotopes is particularly significant during water-rock interactions (e.g., Tipper et al., 2006a, 2006b, 2012a, 2012b; Pogge von Strandmann et al., 2008a, 2008b; Teng et al., 2010; Wimpenny et al., 2010; Ryu et al., 2011, 2016; Huang et al., 2012; Liu et al., 2014; Ma et al., 2015; Lara et al., 2017). Previous studies on silicate weathering profiles showed that soils have heavier δ^{26}Mg values relative to the bedrock, with $\Delta^{26}Mg_{soil\text{-}fluid}$ ranging from 0.05 to 0.4‰ (Teng et al., 2010; Huang et al., 2012; Liu et al., 2014). This is supported by the dissolution experiments on silicate materials, which found that light Mg isotopes are preferentially released into water phases (Wimpenny et al., 2010; Ryu et al., 2016). Detailed studies by Tipper et al. (2006a) and Brenot et al. (2008) showed that soils are isotopically enriched in heavy Mg (−0.11 to 0.02‰) compared to the parent silicate rock (−0.42 to −0.53‰), while corresponding river waters display light Mg isotopic compositions (−0.26 to −0.7‰), suggesting a preference for light Mg isotopes in water phases during silicate weathering.

If only water-rock interactions are considered, soils would be enriched in heavy isotopes in most cases because light Mg isotopes exhibit a preference for water phases. However, previously published δ^{26}Mg data on natural soils displayed a large range from −1.0 to 1.8‰ (data are shown in Supplementary materials, Table S1), many of which are isotopically light relative to bedrock values. Thus, processes at play in soil systems, such as ion exchange, clay mineral transformation, carbonate precipitation, organic matter formation, and external Mg inputs, could significantly accumulate light Mg isotopes (Bolou-Bi et al., 2012; Huang et al., 2012; Opfergelt et al., 2012, 2014; Wimpenny et al., 2014a, 2014b; Ma et al., 2015). For example, Wimpenny et al. (2014a) found that clay minerals preferentially take up isotopically heavy Mg into their structures, but exchangeable Mg displays identical δ^{26}Mg values to corresponding water phases, suggesting that the retention of exchangeable Mg in Mg-depleted clay minerals (e.g., kaolinite) could potentially drive the Mg isotopic compositions of bulk clay minerals to lighter values. This conclusion is similar to that proposed by Opfergelt et al. (2012), who suggested that Mg input from sea spray on soil exchange complexes shifts the bulk soil δ^{26}Mg towards lighter values, counteracting the preferential incorporation of heavy Mg isotopes in secondary clay minerals. Huang et al. (2012) showed that the desorption of heavy Mg isotopes ultimately lead to the retention of light Mg isotopes in soils, even though Mg adsorption in soils favors heavy Mg isotopes. The phase transformation of soil minerals was also suggested to accumulate light Mg isotopes because Mg^{2+} ions with light Mg isotopes from soil waters could be incorporated into the crystal structures of secondary mineral neoformation (Ma et al., 2015). Given the significantly light Mg isotopic compositions in carbonates (e.g., Galy et al., 2002; Li et al., 2012, 2015), carbonate precipitation has also been shown to drive the bulk soil δ^{26}Mg to lighter values (Wimpenny et al., 2014b). In addition, the biological recycling of Mg by vegetation can lower bulk soil δ^{26}Mg values (Tipper et al., 2010; Bolou-Bi et al., 2012).

Supplementary data associated with this article can be found, in the online version, at https://doi.org/10.1016/j.gca.2018.06.028.

Apparently, both the direction and magnitude of Mg isotope fractionation in soil systems are complex, and many factors can modify the Mg isotopic compositions. Notably, the interaction between secondary minerals (e.g., clay minerals and metal oxides) and soil waters is the most critical factor to fractionate Mg isotopes because of the considerably different physicochemical properties (e.g., Mg species,

coordination numbers, and bond length) and the various Mg sources between solid and water phases.

Iron oxides are common natural mineral constituents that are widely distributed in soils, especially in highly matured soils that have formed over much longer periods (e.g., 10^7–10^8 years) (Cornell and Schwertmann, 2003). In some cases, such as hydromorphic environments, Fe oxides can be aggregated and occur as Fe-Mn nodules (FMNs) because of seasonal changes in the redox potential and pH of soils (McKenzie, 1975; Palumbo et al., 2001; Liu et al., 2002; Tan et al., 2005, 2006; Jien et al., 2010; Yu et al., 2015). Because of their high surface/volume ratio, Fe oxides can concentrate and control the distribution and mobility of metals in soils and are thus considered to play a key role in the soil environmental behaviour of metals, including Mg (Childs, 1975; Palumbo et al., 2001; Liu et al., 2002). For example, Sposito (1989) reported a significant increase in concentrations of metals such as Cu, Zn or Cd in the soil waters, which is related to Mn and Fe reduction, and mobilization resulted from the lowered redox potential in flooded soils. Under low redox potentials, Mg^{2+} ions can be released from Fe oxides; under high redox potentials, Mg^{2+} ions are again fixed into Fe oxides (Stoyanovsky and Cederbaum, 1998; Palumbo et al., 2001). Frequently repeated release and incorporation can lead to the net mobility and redistribution of Mg^{2+} ions among Fe oxides, clay minerals, and soil waters. Thus, significant Mg isotope fractionation may occur during these processes. However, to our knowledge, the role of Fe oxides in controlling Mg isotope fractionation in soils remains unclear.

In this study, we systematically investigate the Mg isotopic compositions of FMNs, surrounding soils, soil waters, and soil surface waters in a paddy soil profile, and stream waters, and rainwaters from Guangxi, China. We explore the mechanisms controlling the Mg isotopic compositions of FMNs and surrounding soils. Then, we reveal the implications of Fe oxides in controlling the Mg isotopic compositions of soils. Our findings are expected to help improve our knowledge of the behaviour of Mg isotopes during the formation of Fe oxides and provide implications for the tracing of Mg cycling in soil systems.

2. SITE DESCRIPTION, SAMPLE COLLECTION AND PRETREATMENT

The studied samples were collected in Long'an County, Guangxi Province in southwestern China (107°56′26″E, 23°02′55″N), where karst is widely developed (Fig. 1A). Most carbonate rock outcrops and a large proportion of covered carbonate rocks were karstified over geological timespans. The study site is near the river at a low altitude. The climate in the sample collection area is categorized as a subtropical climate, with a mean annual temperature of 16.5–20.5 °C and mean rainfall of 1389.1 mm (Chen et al., 2010). All the samples were taken from a paddy soil profile with a vertical 90-cm horizon depth (150-cm length × 80-cm width × 90-cm depth; Fig. 1B). The soils in the study area are latosolic red soils, which are derived from the weathering of granites (He et al., 2004). These soils have been used for the double cropping of paddies for more than fifty years.

Samples were collected in July 2016 and January 2018 during the slack-farming season. Four horizons along the profile were classified based on color, organic matter, and particle diameter (Fig. 1B): plough horizon (A, 0–16.5 cm), plow horizon (P, 16.5–40.5 cm), waterloggogenic horizon (W, 40.5–70.5 cm), and parent material horizon (C, 70.5–90 cm). Bulk samples (containing FMNs) from each horizon were collected, immediately sealed in airtight plastic bags, stored frozen in the field, and transported to the laboratory within 24 h. In the lab, these samples were air-dried for 72 h to remove water. FMNs were manually picked from the bulk samples with tweezers, and the remaining soil was denoted as "surrounding soil". The hand-picked FMNs were washed three times with Milli-Q water to remove loose surface particles and then air-dried again to remove water. Afterwards, the FMNs were weighted to calculate the weight percentage in each horizon. The weight percentage data showed that FMNs exhibited different proportions in different horizons (Table 1), with 3.9 wt% in the horizon A, 11.8 wt% in the horizon P, 24.7 wt% in the horizon W, and 15.0 wt% in the horizon C. Rice plants at the topsoil of the profile were sampled and washed with Milli-Q water to remove soil particles. After being transferred to lab, roots, stems, leaves, and grains from the rice plants were separated by ceramic scissors and then dried separately in an oven at 105 °C for 1.5 h and then 75 °C for 48 h. In addition, carbonates and parent granites near the paddy field were collected. Finally, the FMNs, surrounding soils, plants, and rocks were crushed by using an agate mortar and passed through a nylon sieve (<0.25 mm, >200 mesh).

Soil waters that corresponded with these four soil horizons were collected by suction lysimeters, which comprised porous cups and PVC tubes. Soil surface waters were hand-collected in the studied field. Stream waters were collected near the paddy field with auto-samplers. Rainwaters were collected during rainfall. All the water samples were filtered with 0.22-μm nylon filters, acidified with ultrapure HNO_3, and stored in pre-cleaned HDPE bottles at 4 °C.

3. EXPERIMENTAL METHODS

3.1. Key property analysis

Soil pH was measured on surrounding soils in deionized water with 25 mL of solution and 5 g of soil powder. The total soil organic carbon (TOC) content was determined by gas chromatography after dry combustion by using a Thermo Finnigan CHN autoanalyzer. The bulk density of each sample was determined from the measured volume and the sample weight after drying at 105 °C for 24 h. Major elements were measured by inductively coupled plasma optical emission spectroscopy (ICP-OES, Prodigy, U.S.) after digestion through alkaline fusion with lithium metaborate. Trace elements were measured by inductively coupled plasma mass spectrometry (ICP-MS, PerkinElmer, U.S.) through bulk digestion with a mixture of HF-HCl-HNO_3. The mineral composition of FMNs and

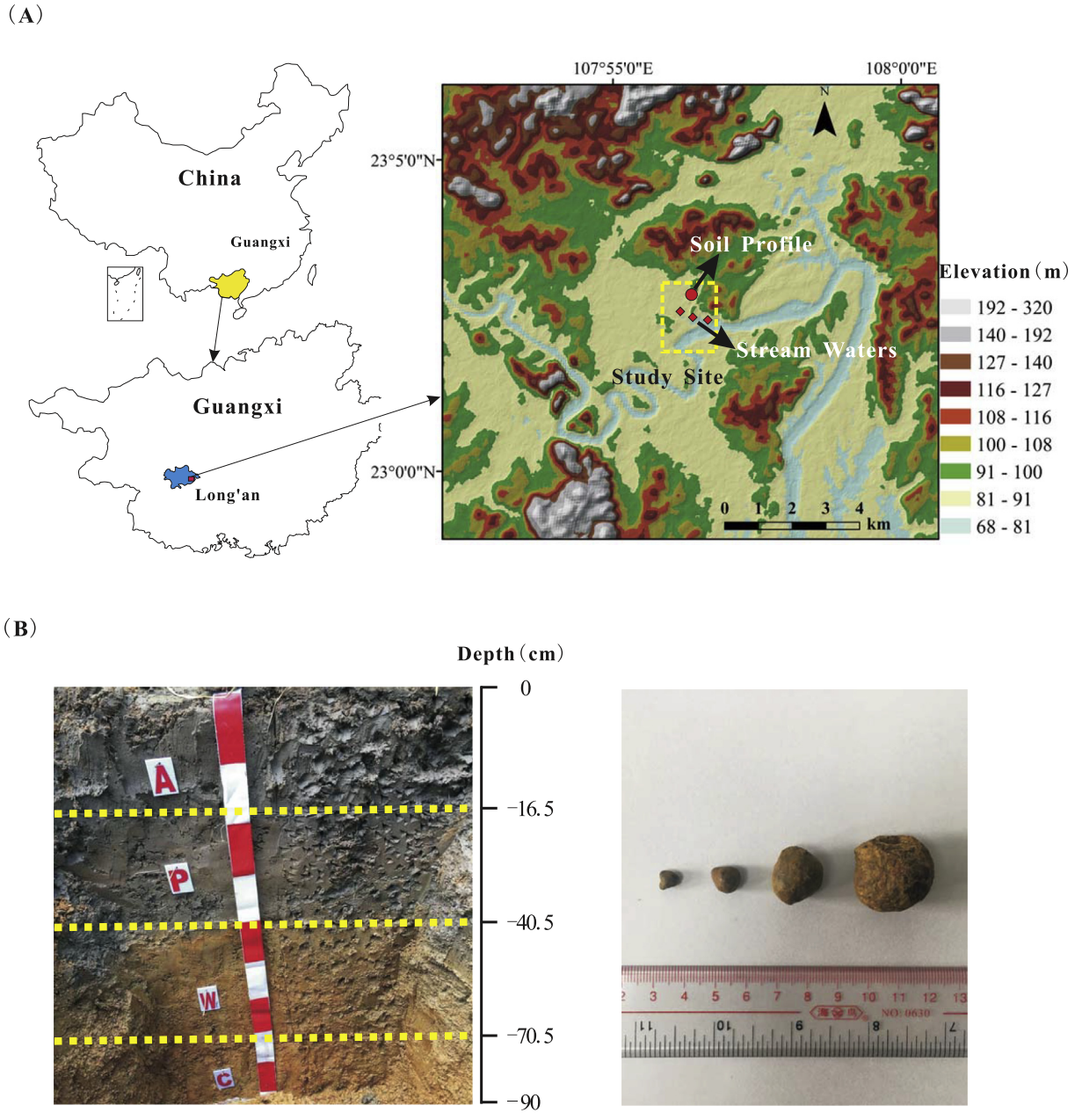

Fig. 1. Photograph and site location map of the paddy soil profile. The red circle and rhombus represent the sampling site in Longan, Guangxi Province, China. The sampling location is characterized by latosolic red soil, which is widely distributed in Guangxi Province. A (0–16.5 cm), plough horizon; P (16.5–40.5 cm), plow horizon; W (40.5–70.5 cm), waterloggogenic horizon; C (70.5–90.0 cm), parent material horizon.

surrounding soils was characterized by an X-ray power diffractometer (Bruker D8, Germany). The X-ray radiation range was 10–90° and the step size was 0.02°, with a scanning speed of 1 s per step. Quantitative analyses of the phase compositions were performed with the Rietveld method by using the TOPAS V4.2 program (Bruker AXS, Mannheim, Germany) based on the XRD pattern of each sample.

3.2. Sequential extraction experiment

Sequential extraction experiments were conducted to separate the exchangeable and structural Mg in FMNs and surrounding soils. Although NH_4-Acetate has been widely employed to liberate exchangeable metals, several researchers suggested that NH_4-Acetate could also attack carbonates (Chapman, 1965; Tessier et al., 1979). According to Chapman (1965), the solubility of $CaCO_3$ is much lower in 1 M Na-Acetate at pH 8.2 than in 1 M NH_4-Acetate at pH 7. For this reason, Na-Acetate (pH = 8.2) has also been commonly used to extract exchangeable metals. Two solutions were tested (NH_4-Acetate, pH = 7; Na-Acetate, pH = 8.2) to determine the best technique to extract the soil exchangeable Mg fraction without releasing carbonate Mg, which may have a different isotopic

Table 1
Key physicochemical properties and mineral compositions of FMNs and surrounding soils.

Horizon	Depth (cm)	pH (H_2O)	Density (g/cm^3)	TOC (g/kg)	Particle distribution		FMN					Surrounding soil			
					FMN	Surrounding soil	Qtz	Gt	Crt	Ill	Cal	Qtz	Ill	Kln	Cal
					(g/kg)	(g/kg)	(wt.%)					(wt.%)			
A	0.0–16.5	7.54	0.83	28.5	39.0	961	8.6	82.0	2.0	1.1	6.3	61.3	5.1	29.1	4.4
P	16.5–40.5	7.68	0.92	20.0	118.4	881.6	10.2	81.6	2.1	1.3	4.7	67.3	4.4	26.3	2.4
W	40.5–70.5	7.85	0.84	3.5	247.3	752.7	16.0	78.9	2.6	2.5	0.0	57.1	4.4	38.5	0.0
C	70.5–90.0	7.40	0.84	2.0	149.9	850.1	9.3	86.4	1.6	2.7	0.0	46.1	5.1	48.8	0.0

Qtz: Quartz; Gt: Goethite; Crt: Cronstedtite; Ill: Illite; Cal: Calcite; Kln: Kaolinite.

signature. The sample LA1-4S, which contained the highest calcite, was used. The results suggested that the concentrations of Ca in these two solutions were identical (Table S2), so the procedure with NH_4-Acetate included significantly limited carbonate Mg.

In this study, 1 M NH_4-Acetate at pH 7 was chosen to extract exchangeable Mg. Approximately 2000 mg of the powdered samples (100–200 mesh) was weighted into 50-mL centrifuge tubes with 20 mL of 1 M NH_4-Acetate (pH = 7), and then the tubes were placed on a shaker and run at 6000 rpm for 1 h at room temperature. After being centrifuged (3600*g*, 20 min) the supernatants in the tubes were decanted and filtered through 0.22-μm nylon filters. To achieve the completed recovery, the same operation was repeated twice more by using MQ water but not NH_4-Acetate. All solutions obtained after each extraction cycle were mixed together and this solution represented the exchangeable Mg, which was denoted as $Mg_{FMN.exch}$ in the FMNs and $Mg_{SS.exch}$ in the surrounding soils. The extracted solutions were evaporated in Teflon beakers on a hotplate and oxidized with H_2O_2 to remove organic matter and then processed to analyze the Mg concentration and Mg isotopic compositions. The residues after extraction were washed three times with Milli-Q water and dried overnight at 105 °C before being grounded to fine powder. Approximately 20 mg of this powder was then completely dissolved through a mixture of HF-HCl-HNO_3 to analyze the total Mg concentration and Mg isotopic composition. This solution represented the structural Mg, which was denoted as $Mg_{FMN.stru}$ in FMNs and $Mg_{SS.stru}$ in the surrounding soils.

3.3. Mg purification and Mg isotope analysis

Magnesium purification for isotope analysis was conducted in a class-1000 clean room at the Isotope Laboratory of the China University of Geosciences (CUGB), Beijing, China. The reagents, which include HF, HCl, and HNO_3, were prepared by sub-boiling distillation. Deionized water (18.2 MΩ), which was prepared on an ultrapure water system of Milli-Q, was used for all the experiments.

The FMNs, surrounding soils, rocks, and plants were digested by using a mixture of concentrated acid in high-pressure Parr digestion vessels. Approximately 20 mg of soil samples and 100 mg of plant samples were weighted into PTFE bomb vessels in a 1:4 (v/v) mixture of concentrated HF-HNO_3. Then, the vessels were sealed with a Parr bomb and placed in a pre-heated oven for 16 h at 180 °C. After naturally cooling, 1–2 mL of 30% H_2O_2 was added and then covered on a hot plate at 70 °C for 1 h to remove organic matter. Afterwards, the clear solution was transferred into Savillex beakers and treated with a 3:1 (v/v) mixture of HCl-HNO_3, followed by heating at 140 °C for 1 to 2 days and then evaporating to dryness at 80 °C. The samples were refluxed with concentrated HNO_3 at 140 °C until complete digestion was achieved and subsequently evaporated to dryness at 80 °C. This dried residue was finally dissolved in 1 N HNO_3 in preparation for ion exchange column chemistry. The soil waters, soil surface waters, rainwaters, stream waters, and extracted solutions were simply

treated by H_2O_2 and a mixture of HF-HCl-HNO_3 before chromatographic separation.

The separation of Mg was achieved through cation exchange chromatography by using AG50W-X8 resin (Bio-Rad 200–400 mesh) in 1 N HNO_3 (Gao et al., 2016; Ke et al., 2016). Considering the high Mn concentration in the FMNs, surrounding soils, extraction residues, and soil waters, an additional chromatographic step was processed to remove Mn. The separation of Mg from Mn was conducted based on Bizzarro et al. (2011) by using Bio-Rad AG50W-X8 resin (200–400 mesh) in 0.5 N HCl-95% acetone media. The geological reference materials BHVO-2, PCC-1, and GSP-2 were processed together with samples for each batch of column chemistry. The same column procedure was repeated twice to obtain a pure Mg solution for mass spectrometry. The total procedural blank was <10 ng, which represented <1‰ of the Mg that was loaded on the column.

The Mg isotopic ratios were determined on a Neptune Plus MC-ICPMS at the CUGB and USTC (University of Science and Technology of China, Hefei) that operated in wet plasma mode with the standard-sample bracketing method (An et al., 2014; Gao et al., 2016; Ke et al., 2016). Prior to analysis, the samples and standards were matched to 400 ppb in 3% HNO_3 at the CUGB and 500 ppb in 2% HNO_3 at the USTC. Measurements were conducted in low resolution mode, and the 1-ppm solution typically yielded a beam intensity of ~15 V at the CUGB and ~25 V at the USTC for ^{24}Mg, with background Mg signals of <10 mv. The standard-sample sequence was repeated four times at the CUGB and three times at the USTC for each sample to achieve better reproducibility. The Mg isotopic compositions of the samples were expressed as deviations between the sample and standard DSM3 (Galy et al., 2003) through $\delta^{x}Mg(‰) = [(^{x}Mg/^{24}Mg)_{sample}/(^{x}Mg/^{24}Mg)_{DSM3} - 1] \times 1000$, where x refers to a mass of 25 or 26. The long-term external reproducibility was <0.06‰ (2SD) for $\delta^{26}Mg$ based on replicate runs of geological reference materials (An et al., 2014; Gao et al., 2016; Ke et al., 2016). The reference material DSM3 yielded $\delta^{26}Mg$ value of -0.05 ± 0.03‰, consistent with the theoretical value of zero within uncertainty. The geological standard materials BHVO-2, PCC-1, and GSP-2 yielded average $\delta^{26}Mg$ values of -0.26 ± 0.04‰, -0.21 ± 0.06‰, and 0.07 ± 0.04‰, respectively, which matched previously published data (e.g., Pogge von Strandmann et al., 2008a; An et al., 2014; Teng et al., 2015, 2017).

4. RESULTS

4.1. Key physicochemical properties and mineral compositions of FMNs and soils

The pH, density, and total organic carbon (TOC) are presented in Table 1 and Fig. 2. The pH and density display a narrow range from 7.40 to 7.85 (Fig. 2A), and from 0.83 to 0.92 g/cm^3 (Fig. 2B), respectively. The TOC of the surrounding soils increases towards the surface horizon, ranging from 2.0 to 28.5 g/kg (Fig. 2C).

The mineral compositions of the FMNs and surrounding soils are presented in Table 1. The FMNs mainly consist of goethite, quartz, illite, calcite and cronstedtite, among which goethite is the dominant mineral, comprising 78.9 to 86.4 wt%. The quartz, illite, and cronstedtite contents vary from 8.6 to 16.0 wt%, from 1.1 to 2.7 wt%, and from 1.6 to 2.6 wt%, respectively. These four minerals show relatively constant contents versus depth within the uncertainties. By contrast, the calcite content increases towards the surface horizon, ranging from 0 to 6.3 wt%.

The surrounding soils mainly consist of quartz, kaolinite, illite, and calcite. The quartz (46.1–67.3 wt%) and calcite (0–4.4 wt%) contents increase from the bottom towards the top of the soil profile. By contrast, the kaolinite content (26.3–48.8 wt%) decrease from the bottom towards the surface horizon. Similar to the FMNs, the illite content in the surrounding soils remains constant throughout the soil profile (Table 1).

4.2. Magnesium distribution

The element concentrations of the FMNs and surrounding soils are reported in Table 2. We calculated the enrichment factor (EF) according to Ahrens et al. (1967) ($EF = C_{FMN}/C_{SS}$, where C refers to the element concentration) to quantitatively evaluate the enrichment ability of the FMNs for an element. The EF data for heavy elements, including Cr, Mn, Cd, Fe, Cu, Zn, and Ni, vary from 1.5 to 9.9, indicating high enrichment ability for these elements

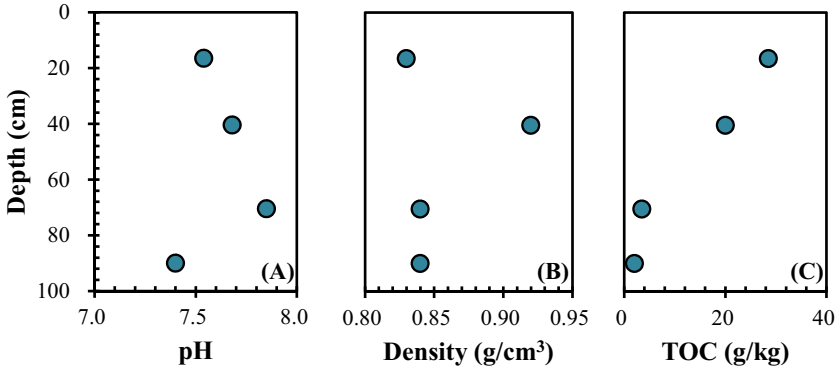

Fig. 2. pH, density and TOC of soils as a function of depth. The data are reported in Table 1.

Table 2
Element concentrations of FMNs, surrounding soils, soil waters, and plants.

Sample name	Horizon	Sample type	Al_2O_3 (%)	Fe_2O_3 (%)	MnO (%)	MgO (%)	CaO (%)	Na_2O (%)	Cr (μg/g)	Ni (μg/g)	Cu (μg/g)	Zn (μg/g)	Cd (μg/g)
LA1-4S	A	Surrounding soil	14.69	6.32	0.07	1.33	2.95	0.31	115.72	74.27	33.07	206.93	1.02
LA1-4F		FMN	13.59	51.63	0.82	0.33	2.91	0.03	939.05	78.34	114.86	531.43	11.14
LA1-3S	P	Surrounding soil	13.62	6.04	0.08	0.91	1.99	0.04	125.80	52.89	32.28	174.12	1.10
LA1-3F		FMN	13.25	54.79	0.92	0.32	1.93	0.03	1182.56	69.40	109.04	468.25	5.45
LA1-2S	W	Surrounding soil	17.95	7.82	0.08	0.54	0.53	0.05	107.95	41.03	30.41	126.42	1.37
LA1-2F		FMN	14.94	51.96	0.37	0.38	0.31	0.03	1062.10	66.78	93.26	395.16	7.91
LA1-1S	C	Surrounding soil	21.28	7.72	0.08	0.58	0.49	0.05	93.18	38.29	30.16	119.72	1.37
LA1-1F		FMN	15.77	48.71	0.68	0.38	0.35	0.03	1149.26	75.90	100.38	435.14	13.13
Sample name	Horizon	Sample type	Al (μg/g)	Fe (μg/g)	Mn (μg/g)	Mg (μg/g)	Ca (μg/g)	Na (μg/g)	Cr (μg/g)	Ni (μg/g)	Cu (μg/g)	Zn (μg/g)	Cd (μg/g)
LA1-5	—	Root	/	/	812.68	1384.60	/	/	15.67	8.97	9.36	41.42	1.31
LA1-6	—	Stem	/	/	125.23	1468.29	/	/	0.92	1.01	0.91	130.68	0.05
LA1-7	—	Leaf	/	/	222.17	1748.59	/	/	2.37	2.27	1.93	132.41	0.05
LA1-8	—	Grain	/	/	23.32	1101.08	/	/	1.17	0.77	0.72	19.05	0.01

"—" represents the inexistence, and "/" represents no measurement.

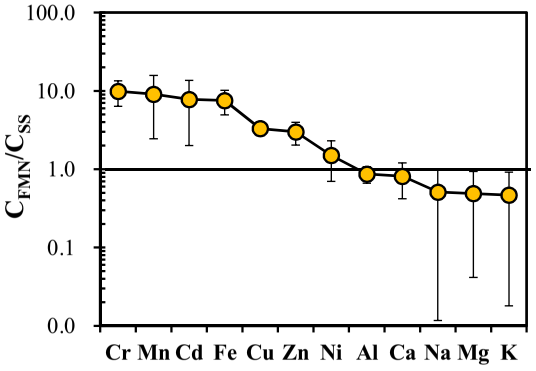

Fig. 3. Average EFs of elements in FMNs relative to surrounding soils. EF ($EF = C_{FMN}/C_{SS}$) was calculated according to Ahrens et al. (1967).

in the FMNs (Fig. 3). By contrast, the FMNs do not show such an enrichment ability for Al, Ca, Na, Mg, and K, of which the EF values are all lower than 1. The EF values for Mg range from 0.25 to 0.70 along the profile, with an average value of 0.49 ± 0.45. The FMNs have a uniform MgO content (0.33–0.38 wt%) along the profile (Fig. 4A). Compared to the FMNs, the surrounding soils along the profile have different MgO contents from 0.54 to 1.33 wt %, which are higher than those in the FMNs. The distribution of exchangeable and structural Mg in the FMNs and

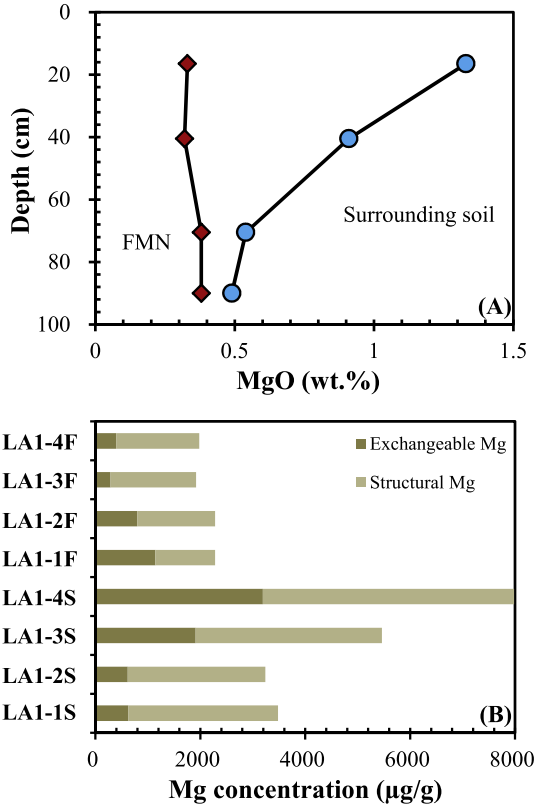

Fig. 4. MgO contents of FMNs and surrounding soils as a function of depth (A), and Mg concentration in different Mg pools in FMNs and surrounding soils (B).

surrounding soils is presented in Fig. 4B. A high concentration of exchangeable Mg is found in the FMNs in the W (798 μg/g) and C (1140 μg/g) horizons, whereas low concentrations are found in the A (396 μg/g) and P (288 μg/g) horizons. Conversely, the surrounding soils in the A (3192 μg/g) and P (1911 μg/g) horizons contain higher concentrations of exchangeable Mg relative to the W (616 μg/g) and C (626 μg/g) horizons.

4.3. Magnesium isotopic compositions

The Mg isotopic compositions of the total Mg in different media from the soil profile, including FMNs, surrounding soils, parent granites, carbonates, soil waters, vegetation, stream waters, soil surface waters, and rainwaters, are presented in Table 3. The Mg isotopic compositions of exchangeable Mg and structural Mg are shown in Table 4. The Mg isotopic compositions of all the samples fall along a single mass-dependent fractionation line, which has a slope of 0.515, on the three-isotope diagram (Fig. S1), close to the theoretical equilibrium and kinetic fractionation values (0.521 and 0.511, respectively) (Young and Galy, 2004).

The Mg isotopic compositions of the bulk FMNs range from −1.39 to −1.58‰ (Fig. 5), with an average value of −1.47 ± 0.16‰. Compared to the parent granites (−0.25 ± 0.04‰), the surrounding soils have lighter Mg isotopes, ranging from −0.59 to −0.85‰ (Fig. 5) with an average δ^{26}Mg value of −0.71 ± 0.27‰. The average difference in the δ^{26}Mg values between the FMNs and surrounding soils is 0.76 ± 0.14‰. In both of the FMNs and surrounding soils, the exchangeable Mg exhibits the lightest δ^{26}Mg values within a similar range (−1.79 to −2.15‰ in the FMNs, and −1.62 to −1.91‰ in the surrounding soils) (Fig. 6A and B), with an average value of −1.91 ± 0.33‰ and −1.82 ± 0.34‰, respectively. By contrast, structural Mg has the heaviest δ^{26}Mg values (−1.21 to −1.33‰ in the FMNs, and −0.27 to −0.38‰ in the surrounding soils), with an average value of −1.28 ± 0.10‰ and −0.34 ± 0.09‰, respectively. The excellent agreement between the measured and calculated total Mg isotope data (Fig. S2) suggests that Mg loss, which could be expected due to the incomplete recovery of extracted solutions during the sequential extraction procedure, did not occur.

The soil waters are characterized by a homogeneous Mg isotopic composition (−1.65 to −1.55‰) throughout the soil profile (Fig. 5), with an average value of −1.59 ± 0.09‰, which is heavier than the exchangeable Mg in the FMNs and surrounding soils. The soil surface waters (−1.56 to −1.59‰) and rainwaters (−1.46 to −1.52‰)

Table 3
Magnesium isotopic compositions for standards, FMNs, surrounding soils, soil water and plants.

Sample name	Horizon	Sample	δ^{25}Mg	2SD	δ^{26}Mg	2SD	N
LA1-4S	A	Surrounding soil	−0.43	0.05	−0.85	0.03	4
LA1-4F		FMN	−0.70	0.04	−1.39	0.02	4
LA1-4P		Soil water	−0.85	0.03	−1.65	0.04	3
LA1-3S	P	Surrounding soil	−0.41	0.05	−0.81	0.02	4
LA1-3F		FMN	−0.76	0.05	−1.48	0.02	4
LA1-3P		Soil water	−0.82	0.05	−1.60	0.04	3
LA1-2S	W	Surrounding soil	−0.33	0.02	−0.61	0.03	4
LA1-2F		FMN	−0.74	0.04	−1.45	0.06	4
LA1-2P		Soil water	−0.83	0.02	−1.57	0.05	3
LA1-1S	C	Surrounding soil	−0.30	0.02	−0.59	0.01	4
LA1-1F		FMN	−0.80	0.03	−1.58	0.04	4
LA1-1P		Soil water	−0.80	0.02	−1.55	0.04	3
LA1-5	—	Root	−0.35	0.04	−0.67	0.02	4
LA1-6	—	Stem	−0.50	0.03	−0.98	0.04	4
LA1-7	—	Leaf	−0.60	0.02	−1.17	0.01	4
LA1-8	—	Grain	−0.34	0.03	−0.67	0.05	4
LA1-9	—	Granite	−0.13	0.04	−0.25	0.04	4
LA1-10	—	Carbonate	−1.66	0.03	−3.23	0.05	4
LA1-1R	—	Stream water	−0.70	0.04	−1.37	0.05	3
LA1-2R	—	Stream water	−0.68	0.02	−1.32	0.02	3
LA1-3R	—	Stream water	−0.74	0.03	−1.45	0.03	3
LA1-1B	—	Surface water	−0.82	0.05	−1.56	0.01	3
LA1-2B	—	Surface water	−0.84	0.04	−1.59	0.03	3
LA1-1Y	—	Rainwater	−0.79	0.06	−1.52	0.04	3
LA1-2Y	—	Rainwater	−0.77	0.06	−1.46	0.04	3
LA1-3Y	—	Rainwater	−0.78	0.05	−1.50	0.08	3
PCC-1	—	Peridotite	−0.11	0.06	−0.21	0.04	4
GSP-2	—	Granite	0.03	0.04	0.07	0.04	3
BHVO-2	—	Basalt	−0.12	0.04	−0.26	0.04	4
DSM3	—	Mg solution	−0.04	0.03	−0.05	0.03	4

"N" represents the number of repeated analyses of the same solution by MC-ICPMS. 2SD = 2 times the standard deviation of population analyzed. "—" represents the inexistence.

Table 4
Magnesium concentrations and Mg isotopic compositions of bulk, exchangeable, and structural Mg from FMNs and surrounding soils.

Sample name	Horizon	Mg pools	Mg conc. (μg/g)	δ^{25}Mg (‰)	2SD	δ^{26}Mg (‰)	2SD	N
LA1-4S	A	Structural	4788	−0.18	0.03	−0.34	0.05	4
		Exchangeable	3192	−0.83	0.05	−1.62	0.06	4
LA1-3S	P	Structural	3549	−0.19	0.05	−0.36	0.05	4
		Exchangeable	1911	−0.91	0.06	−1.74	0.06	4
LA1-2S	W	Structural	2624	−0.19	0.05	−0.38	0.03	4
		Exchangeable	616	−1.03	0.01	−2.00	0.05	4
LA1-1S	C	Structural	2854	−0.14	0.02	−0.27	0.06	4
		Exchangeable	626	−0.98	0.08	−1.91	0.10	4
LA1-4F	A	Structural	1584	−0.61	0.08	−1.21	0.08	4
		Exchangeable	396	−0.98	0.08	−1.91	0.02	4
LA1-3F	P	Structural	1632	−0.68	0.03	−1.33	0.06	4
		Exchangeable	288	−1.10	0.05	−2.15	0.05	4
LA1-2F	W	Structural	1482	−0.66	0.04	−1.29	0.04	4
		Exchangeable	798	−0.94	0.04	−1.81	0.07	4
LA1-1F	C	Structural	1140	−0.68	0.05	−1.30	0.07	4
		Exchangeable	1140	−0.92	0.05	−1.79	0.07	4

"N" represents the number of repeated analyses of the same solution by MC-ICPMS. 2SD = 2 times the standard deviation of population analyzed.

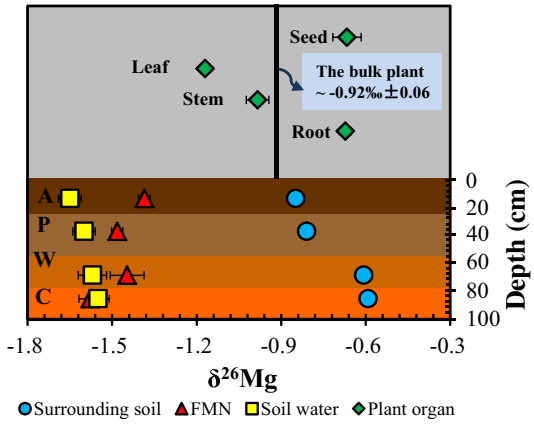

Fig. 5. Magnesium isotopic compositions of FMNs, surrounding soils, soil waters and plants.

show similar δ^{26}Mg values to those of the soil waters, with an average value of -1.58 ± 0.04‰ and -1.49 ± 0.06‰, respectively. Compared to the soil waters, the stream waters have slightly heavier Mg isotopic compositions (−1.32 to −1.45‰), with an average value of -1.38 ± 0.13‰.

The Mg isotopic composition of the rice plants varies as a function of different plant organs (Fig. 5), decreasing from the roots (−0.67‰) to the stems (−0.98‰) and leaves (−1.18‰) but increasing from the leaves to the grains (−0.67‰). The Mg isotopic composition of the bulk rice plants ($\delta^{26}Mg_{plant}$) could be calculated by using Eq. (1):

$$\delta^{26}Mg_{plant} = \frac{\sum \delta^{26}Mg_{organ} \times [Mg]_{organ} \times f_{organ}}{\sum [Mg]_{organ} \times f_{organ}}, \quad (1)$$

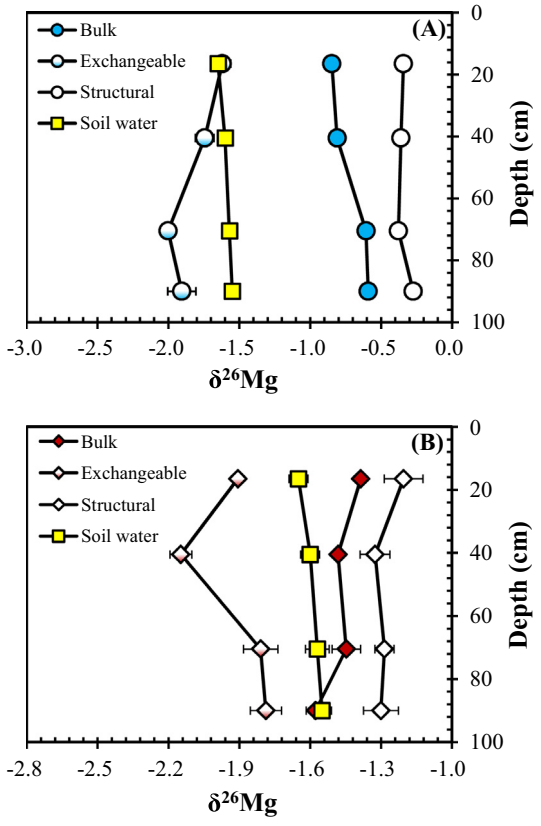

Fig. 6. Magnesium isotopic compositions of the bulk, exchangeable Mg, structural Mg, and soil waters as a function of depth in surrounding soils (A) and FMNs (B) along the soil profile.

where $[Mg]_{organ}$ and $\delta^{26}Mg_{organ}$ are the Mg concentrations and $\delta^{26}Mg$ values of organs, respectively, and f_{organ} is the weight proportion in the total plant. The calculated $\delta^{26}Mg$ value in the bulk plants is −0.92‰, heavier than that in the soil waters but lighter than that in the surrounding soils.

5. DISCUSSION

5.1. Controls on the Mg and $\delta^{26}Mg$ of the surrounding soils

The Mg content in the surrounding soils shows a clear trend with depth, progressively increasing from the bottom to the top of the soil profile (Fig. 4). By contrast, the Mg isotopic compositions follow the opposite trend, ranging from −0.59 to −0.85‰ (Fig. 5A). Furthermore, the Mg isotopic compositions are evidently lighter than that of the parent granite (−0.25‰), with $\Delta^{26}Mg_{granite\text{-}soil} > 0.34$‰. This phenomenon contrasts with the partitioning of Mg into secondary clay minerals, with the preferential loss of light isotopes to fluids and accumulation of heavy isotopes in weathered residues (Teng et al., 2010; Huang et al., 2012; Opfergelt et al., 2012; Liu et al., 2014; Wimpenny et al., 2014a). Such results can be explained by four possible mechanisms: (*i*) the influence of sea spray and eolian inputs; (*ii*) the biological recycling of Mg by vegetation, which adds light Mg isotopes into soils; (*iii*) the contribution of light Mg isotopes from carbonates; and (*iv*) the accumulation of light Mg isotopes in exchangeable sites of Mg-depleted clay minerals.

5.1.1. Influence of sea spray and eolian inputs

Sea spray inputs were suggested to affect the Mg isotopic compositions of soils (Opfergelt et al., 2012, 2014). Seawater exhibits light and homogenous Mg isotopic composition (−0.8 ± 0.1‰) (Foster et al., 2010; Ling et al., 2011), which is significantly heavier than that of soil exchangeable Mg (−2.15 to −1.62‰). Thus, the contribution from sea spray could be limited because a seawater-like Mg isotopic composition could be expected for exchangeable Mg if this contribution is great, as suggested in Opfergelt et al. (2014). Eolian inputs were also shown to modify the Mg isotopic compositions of soils (Liu et al., 2014). However, the similar Mg isotopic compositions between the structural Mg and parent granites indicate that the contribution from eolian dust is very small. On the other hand, the light Mg isotopic compositions in the underlying horizons (P, W, and C) further suggest limited contributions from eolian dust.

5.1.2. Magnesium recycling induced by vegetation

Magnesium is an essential nutrient for plant growth, and vegetation results in the recycling of element Mg in soil systems (Wilkinson et al., 1990; Montezano et al., 2013). The available Mg^{2+} ions, i.e., exchangeable and dissolved Mg, in soils are taken up by roots and stored in vegetation. After being affected by the physiological processes in plants for several months or years, Mg^{2+} ions are released back into soils via secretion and decay. These biological processes could potentially modify the Mg isotopic compositions of soils. Different organs in the rice plants had heavier Mg isotopic compositions than that of the soil waters and soil exchangeable fractions (Fig. 5). As suggested in Bolou-Bi et al. (2012), this result occurs because of the preferential uptake of heavy Mg isotopes by plant roots. However, the plant-available Mg^{2+} in soils (dissolved and exchangeable Mg) is significantly enriched in light Mg isotopes (<−1.5‰), so the $\delta^{26}Mg$ value of the bulk rice plants (−0.92‰) is still lighter than that of the surrounding soils, even though heavier isotopes are preferentially taken up by plants. The TOC content shows an increasing trend towards the surface horizon (Fig. 2C). In addition, it is positively correlated with the MgO content and negatively correlated with the $\delta^{26}Mg$ value (Fig. 7). Thus, lighter Mg isotopes may accumulate in soils when paddy organs such as leaves fall in the surface soils.

Although possible, such a mechanism may only play a minor role in the overall soil Mg isotope fractionation based on mass balance calculations. The highest TOC observed in the surrounding soils is 28.5 g C kg^{-1} (Table 1). Given the Mg concentration of 1426 μg Mg g^{-1} C in organic matter (estimated from the average Mg concentration in the bulk rice plants), only ~0.004 wt% Mg in soils could be associated with organic matter. This value is limited compared to the bulk Mg content in the surrounding soils (average Mg content = 0.5 wt%, Table 1). In addition,

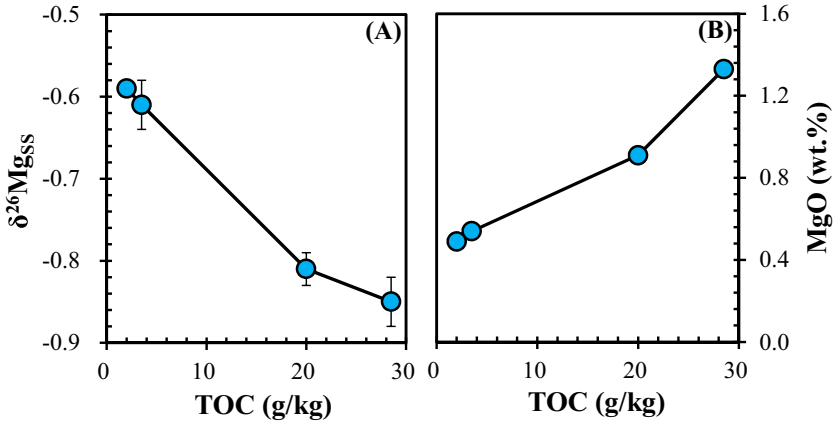

Fig. 7. TOC as a function of the $\delta^{26}Mg_{SS}$ and MgO content.

the two underlying soil samples from the W and C horizons, which contained almost no organic matter, still showed significantly lighter Mg isotopic compositions compared to the parent granite. In this case, bio-recycling is unlikely to be responsible for the accumulation of light Mg isotopes in the surrounding soils.

5.1.3. Carbonate contribution

Carbonate minerals are usually enriched in light Mg isotopes (e.g., Galy et al., 2002; Li et al., 2012; Saenger and Wang, 2014; Ma et al., 2018), and the presence of carbonates in the surrounding soils would drive the soil $\delta^{26}Mg$ to lighter values. For example, studies on loess showed a negative correlation between $\delta^{26}Mg$ values and CaO contents (Huang et al., 2013; Wimpenny et al., 2014b), which was explained by carbonate minerals in loess contributing light Mg isotopes to the bulk loess. Similarly, Wang et al. (2015) demonstrated that carbonates in mudrocks cause the bulk rocks to become significantly enriched in isotopically light Mg. The XRD analysis results in our study show that calcite exists in the surrounding soils, while dolomite is absent (Fig. S3). The calcite contents increase from the bottom to the top of the soil profile (Fig. 8A), which matches the increasing CaO content throughout the soil profile (Fig. 8B). Additionally, the MgO content is positively correlated with the CaO content (Fig. 8C), likely suggesting that the Mg in the surrounding soils is overwhelmingly controlled by calcite. Calcite in soils is thus expected to drive the bulk surrounding soil being enriched in light Mg isotopes. As our study shows, the Mg isotopic compositions of the surrounding soils are lighter with higher calcite contents (Fig. 8D). A simple calculation was conducted to test if calcite could cause such variations in the MgO contents and $\delta^{26}Mg$ values through $\delta^{26}Mg_{calculated\ SS.} = \delta^{26}Mg_{SS.C} + \delta^{26}Mg_{calcite} \times f_{calcite}$ (2) and $[Mg]_{calculated\ SS.} = [Mg]_{SS.C} + [Mg]_{calcite}$ (3), where $\delta^{26}Mg_{SS.C}$ and $[Mg]_{SS.C}$ refer to the Mg isotopic composition and Mg content in the horizon C, respectively. $f_{calcite}$ refers to the proportion of Mg content. In this modeling calculation, we used the MgO content and $\delta^{26}Mg$ value of horizon C as the starting parent material because these values are the most representative with the least external influence. The $\delta^{26}Mg_{calcite}$ was adopted as −3.23‰, the carbonate value in our study area. The modeled results show that the low-Mg calcite in the surrounding soils could drive the soil $\delta^{26}Mg$ to light values (Fig. S4A). However, calcite could not explain such a variation in the MgO contents because the MgO contents do not meet the correspondingly modeled lines (Fig. S4B). The reasons for these results could be that (*i*) the calcite content in soils is very low, ranging from 2 to 5%, and (*ii*) low-Mg calcite contains very low Mg (<5 mol% $MgCO_3$). On the other hand, the two underlying soil samples from the W and C horizons that do not contain calcite still show lighter Mg isotopic compositions relative to the parent

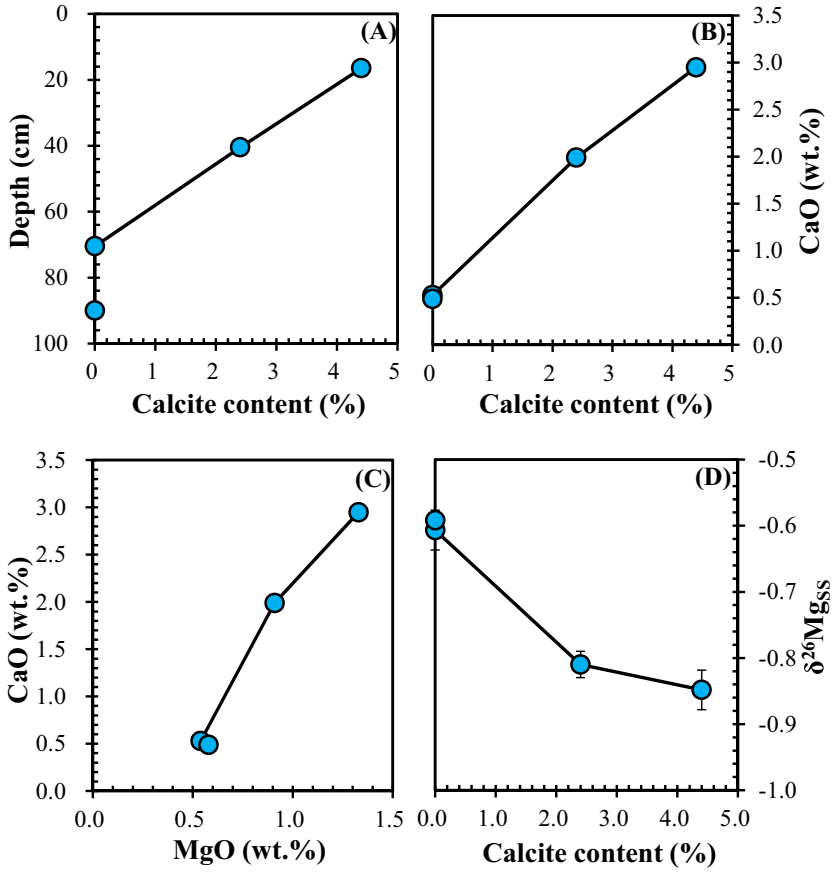

Fig. 8. Calcite content as a function of depth (A), CaO (B), and $\delta^{26}Mg_{SS}$ (D); MgO content as a function of CaO (C).

granite. Therefore, calcite is unlikely to be the dominant mechanism that causes the accumulation of light Mg isotopes in the surrounding soils.

5.1.4. Retention of light Mg isotopes in exchangeable sites of Mg-depleted clay minerals

The retention of light Mg isotopes in exchangeable sites of Mg-depleted clay minerals can potentially explain the light Mg isotopic compositions in the surrounding soils. Considering the different $\delta^{26}Mg$ values for structural Mg and exchangeable Mg, the Mg isotopic composition of the surrounding soils ($\delta^{26}Mg_{SS}$) could be expressed by the mass balance $\delta^{26}Mg_{SS} = \delta^{26}Mg_{SS.stru} \times f_{SS.stru} + \delta^{26}Mg_{SS.exch} \times f_{SS.exch}$ (4) and $f_{SS.stru} + f_{SS.exch} = 1$ (5), where $\delta^{26}Mg_{SS.stru}$ and $\delta^{26}Mg_{SS.exch}$ refer to the Mg isotopic compositions of structural Mg and exchangeable Mg, respectively. $f_{SS.stru}$ and $f_{SS.exch}$ refer to the proportions of Mg in these two Mg pools, respectively. Eqs. (4) and (5) indicate that the soil Mg isotopic compositions depend on the balance between structural and exchangeable Mg and the Mg isotopic composition in these two Mg pools. The extraction experimental results show that the $\delta^{26}Mg$ values of exchangeable Mg are always isotopically lighter (>1.3‰) than those of the structural Mg (Fig. 6A). The results are consistent with those in a previous report, which concluded that $\delta^{26}Mg_{exch}$ is >1.5‰ lighter than $\delta^{26}Mg_{stru}$ in kaolinite, illite and montmorillonite (Wimpenny et al., 2014a). These findings can be potentially used to explain why the surrounding soils have such light Mg isotopic compositions. If massive Mg was reserved in exchangeable sites of clay minerals, then the exchangeable Mg could drive the bulk soil $\delta^{26}Mg$ towards lighter values. A similar phenomenon was observed by Opfergelt et al. (2012), who demonstrated that the retention of light Mg isotopes on soil exchange complexes shifted the bulk soil $\delta^{26}Mg$ towards lighter values.

Pogge von Strandmann et al. (2008a, 2012) and Huang et al. (2012) presented soils that are consistently enriched in light Mg isotopes compared to their parent rocks. In each case, the soil contains a highly Mg-depleted clay mineral such as kaolinite or allophane that have a high proportion of Mg in their exchangeable sites. Furthermore, an experimental study suggested that kaolinite has isotopically light $\delta^{26}Mg$ values compared to illite and montmorillonite because kaolinite contains higher proportions of exchangeable Mg^{2+} ions than illite and montmorillonite (Wimpenny et al., 2014a). This result implies that exchangeable Mg can significantly drive the bulk clay $\delta^{26}Mg$ towards lighter values, and the extent to which the $\delta^{26}Mg$ values of bulk clay are controlled by adsorbed Mg depends on the proportions of exchangeable to structural Mg in the clay. Kaolinite is an Mg-depleted clay mineral that contains a low concentration of Mg, with most of the Mg bound to pH-dependent functional groups on the clay surface (Drever, 1988; Kim et al., 1996; Merkel and Planer-Friedrich, 2008). Our results show that kaolinite comprises a large proportion (ca. 29–49%) in the surrounding soils (Table 1). In addition, the pH values along the profile varies from 7.40 to 7.85 (Table 1), which are significantly higher than the point of zero charge of kaolinite (pH_{PZC} = 2.53–3.56; Scroth and Sposito, 1997). These results suggest that the large amounts of Mg^{2+} ions in the surrounding soils could exist in kaolinite in an exchangeable form. The extraction experimental results show that the proportion of exchangeable Mg increases from the bottom to the top of the soil profile and is negatively correlated with the $\delta^{26}Mg$ value (Fig. 9). Thus, the lighter $\delta^{26}Mg$ values in the surrounding soils than in the parent rocks likely resulted from the retention of large amounts of isotopically light Mg in exchangeable sites in kaolinite.

It's worth noting that the exchangeable Mg concentration was negatively correlated with the abundance of kaolinite. These observations are contradictory to our explanation because the exchangeable Mg concentration would be positively correlated with the abundance of kaolinite if kaolinite accumulated a large amount of Mg^{2+} ions in its exchangeable sites. Such a contradiction could be explained by two possibilities: (*i*) a difference in the adsorption capacity of kaolinite in different soil horizons, and (*ii*) undersaturation with respect to metal ions in kaolinite. The adsorption of ions onto kaolinite strongly depends on the pH value (Kosmulski, 2006). Given the nearly consistent pH value throughout the soil profile (Table 1), the adsorption capacity in different soil horizons

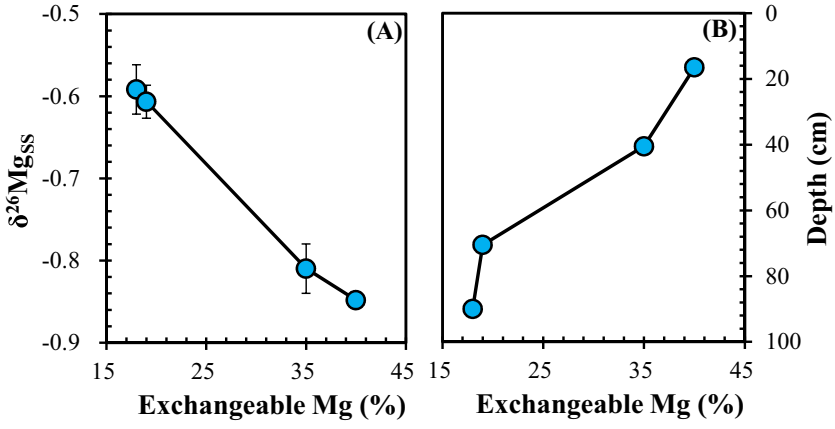

Fig. 9. Proportion of exchangeable Mg as a function of $\delta^{26}Mg$ (A) and depth (B).

could be comparable. Alternatively, undersaturation with respect to metal ions in kaolinite could have produced such results. As discussed above, kaolinite has large adsorption capacity for metal ions because of the significantly higher pH values than its pH_{PZC}. Because of the considerably high enrichment factor for metals ions (Fig. 3), large amounts of metal ions have already been adsorbed on the FMNs (see Section 5.2), causing the surrounding soils to become depleted in metal ions. These two processes cause the kaolinite to become undersaturated with respect to metal ions. Exchangeable Mg is mainly derived from external inputs such as natural waters (discussed in Section 5.3), so the Mg concentration and Mg isotopic compositions in the surrounding soils are most likely related to the depth, i.e., lower depth with higher Mg concentration and lighter Mg isotopes.

5.2. Controls on the Mg and δ^{26}Mg of the FMNs

FMNs are important components in soils and are suggested to predominantly control the distribution and mobility of soil metals (Gasparatos et al., 2012). Trace metal cations (e.g., Cu, Ni, Zn, Cr, Cd, Mo, etc.) are prone to being adsorbed onto the surfaces (adsorption) or enter into the crystal structure (absorption) of FMNs because of their high enrichment abilities for metals (Palumbo et al., 2001; Tan et al., 2005; Gasparatos et al., 2012; the general word "sorption" was used to include both of these mechanisms here). The FMNs in our study also had high affinities for metal cations, in which the average concentrations of Cu, Ni, Zn, Cr, and Cd were ca. 3.3, 1.5, 3.0, 9.9, and 7.8 times higher, respectively, than those in the surrounding soils (Fig. 3). By contrast, Mg do not show such a special affinity for FMNs, of which the average Mg concentration is half that in the surrounding soils. This result matches previously published data, which suggested that Mg in soil FMNs is lower than that in surrounding soils (Palumbo et al., 2001; Tan et al., 2005; Gasparatos et al., 2012). Goethite comprised 79–86% (Table 1) and no Mn oxides are present, suggesting that goethite is the dominant control on metal cations in the FMNs. Large metal stable isotope fractionation has been observed during the sorption of aqueous ions, e.g., Cu and Zn, onto Fe oxides (Pokrovsky et al., 2005, 2008; Balistrieri et al., 2008; Juillot et al., 2008). For example, Balistrieri et al. (2008) documented that Cu and Zn isotopes are significantly fractionated ($\Delta^{65}Cu_{sorbed\text{-}aqueous} = 0.52‰$ and $\Delta^{66}Zn_{sorbed\text{-}aqueous} = 0.73‰$) when sorbed onto amorphous Fe oxyhydroxide. Similar results were found in other reports (Pokrovsky et al., 2005, 2008; Juillot et al., 2008). In all these cases, heavier isotopes are preferentially sorbed onto the Fe oxides compared to the aqueous solution. Such an isotope fractionation of these metals reflects the difference in bond strength between dissolved and adsorbed metals, with heavier isotopes preferentially partitioning into a stronger bonding environment (e.g., lower coordination number; Schauble, 2004).

Similarly to Cu and Zn isotopes, the Mg in the FMNs also exhibits heavier isotopic compositions (−1.39 to −1.58‰; Fig. 5) compared to the dissolved Mg (ave. $\delta^{26}Mg_{soil\ \ water} = -1.59‰$) and the soil exchangeable Mg (ave. $\delta^{26}Mg_{SS.exch.} = -1.82‰$), the main Mg sources in the FMNs. This suggests that the heavier Mg isotopes are preferentially taken up by the FMNs. The Mg isotopes in the FMNs are considerably fractionated among the different Mg forms, with δ^{26}Mg values in the order of structural Mg > exchangeable Mg (Fig. 6B). In all cases, the δ^{26}Mg values of the soil waters are lighter than that of the structural Mg but heavier than that of the exchangeable Mg. This result suggests that the heavy Mg isotopic compositions in the FMNs could be attributed to the preferential incorporation of heavy Mg isotopes into structural sites of Mg-bearing minerals. Illite was shown to contain high Mg concentrations because of the isomorphic exchange of Mg^{2+} for Al^{3+} in the octahedral layer (Appelo and Postma, 2005). However, the very low illite content in the FMNs suggests that the isotope contribution from illite could be negligible. Instead, the mineral constituent of goethite is likely responsible for the isotopically heavy Mg in structural sites of the FMNs. Although few studies have directly focused on the behaviour of Mg during goethite precipitation, Paikaray et al. (2018) suggested that Mg^{2+} can substitute for Al^{3+} and Fe^{3+} during the precipitation of hydroxides, which may also occur in other hydroxides or oxides such as goethite. The Mg^{2+} ions in aqueous solution are octahedrally coordinated with H_2O molecules, forming an octahedral aquo ion $[(Mg(H_2O)_6)]^{2+}$ with an Mg—O length of 2.08 Å (Pavlov et al., 1998; Li et al., 2011, 2014). To our knowledge, no available data have been reported so far for Mg that has been incorporated into the goethite structure. Thus, we utilize the Fe coordination geometry to explain the structural incorporation of Mg because Mg^{2+} has a similar ionic radius as Fe^{3+} in an octahedral structure (0.72 Å for Mg^{2+}, 0.65 Å for Fe^{3+}; Shannon and Prewitt, 1969) and because Mg^{2+} can replace structural Fe^{3+} in goethite via isomorphous substitution with H^+ or vacancies in the cation site (Kinniburgh et al., 1976; Baltpurvins et al., 1997). The Fe—O bond length in goethite (~2.01 Å; Changela et al., 2012) is shorter than the Mg—O bond length (2.08 Å; Pavlov et al., 1998) in aqueous solution. If Mg^{2+} substitutes for octahedral Fe^{3+} in goethite, structural Mg should have considerably heavier Mg isotopic composition than dissolved Mg because the shorter Mg—O bonds strongly favor heavy isotopes relative to longer bonds (Urey, 1947; Schauble, 2004). Nickel isotope fractionation was once suggested to have similar characteristics during its incorporation into the ferrihydrite structure, in which the substitution of octahedral Ni^{2+} for tetrahedral Fe^{3+} in the ferrihydrite structure drives the bulk ferrihydrite Ni towards isotopically heavier values (Wang and Wasylenki, 2017). Therefore, a similar isotopic offset might be expected when Mg^{2+} is substituted for Fe^{3+} in goethite because of the identical ionic radii of octahedral Mg^{2+} (0.72 Å) and Ni^{2+} (0.70 Å) (Shannon and Prewitt, 1969).

Further evidence for supporting the preferential incorporation of heavier Mg isotopes into goethite is the isostructure of goethite (α-FeOOH) and diaspore (α-AlOOH) (Cornell and Schwertmann, 2003). Although Mg isotope fractionation during Mg incorporation into diaspore has never been reported, one study that was conducted

with gibbsite ($Al(OH)_3$) suggested that gibbsite preferentially incorporates heavy Mg isotopes (Liu et al., 2014). Al^{3+} ions in gibbsite and diaspore are both octahedrally coordinated. Additionally, gibbsite and diaspore have an Al—O length of 1.92 Å (Ladeira et al., 2001) and 1.85–1.98 Å (Cabaret et al., 1996), respectively, which are both shorter than the Mg—O length of 2.08 Å in $[(Mg(H_2O)_6)]^{2+}$. Therefore, Mg^{2+} substitution for structural Al^{3+} in both gibbsite and diaspore is most likely to be enriched in heavy Mg isotopes compared to aqueous solution. In this case, Mg^{2+} substitution for structural Fe^{3+} in goethite should preferentially take up heavy Mg isotopes because goethite has a similar structure to diaspore.

The theoretical geometry in our study revealed the preferential incorporation of heavy Mg isotopes into crystal structures, and the Mg bound into structural sites of the FMNs is isotopically heavier than that in the soil waters. However, the isotope fractionation mechanism that is related to the exact Mg coordination geometry in the crystals should be examined in the future through theoretical calculations and a structural analysis method such as synchrotron EXAFS/XANES characterization.

5.3. Contrasts between the FMNs and surrounding soils

5.3.1. Exchangeable Mg

The similarity between the FMNs and surrounding soils was that the exchangeable Mg in both of them exhibited extremely light Mg isotopic compositions, with the $\delta^{26}Mg$ ranging from −2.15 to −1.62‰ (Fig. 6). This range is consistent with the observed $\delta^{26}Mg$ values of exchangeable Mg in illite (−1.73‰), kaolinite (−1.77‰), and montmorillonite (−1.72‰) (Wimpenny et al., 2014a). Such light Mg isotopic compositions likely reflect a fluid phase (Wimpenny et al., 2014a) because clay minerals and Fe oxides can be exposed to natural waters (e.g., stream waters and rainwaters), and long-term interactions may result in massive amounts of Mg^{2+} ions being adsorbed onto these minerals in an exchangeable form. The stream waters and rainwaters in our study area have $\delta^{26}Mg$ values from −1.32 to −1.59‰, which are identical to those in rivers that drain carbonates (Tipper et al., 2006a; Brenot et al., 2008; Jacobson et al., 2010). This result suggests that carbonates could be the dominant source that contributes light Mg isotopes to the exchangeable Mg in the FMNs and surrounding soils

The exchangeable Mg in soil-FMN systems reflects a fluid phase, so their $\delta^{26}Mg$ values should be consistent with those of the soil waters. Interestingly, the $\delta^{26}Mg$ values of exchangeable Mg are still lighter than that of the soil waters (Fig. 6), with an average $\delta^{26}Mg$ difference of 0.28‰. Thus, additional processes, alongside the input of carbonate-bearing river waters, may have further lowered the Mg isotopic compositions of exchangeable Mg. Given the open system and agricultural use of the studied soils, atmospheric and anthropogenic inputs can potentially lower the $\delta^{26}Mg$ values of exchangeable Mg. However, soil surface waters (−1.45 to −1.59‰) that are contaminated by fertilizers and rainwaters (−1.46 to −1.52‰) have identical $\delta^{26}Mg$ values to the soil waters, so atmospheric and anthropogenic inputs do not likely influence the soil exchangeable Mg.

Instead, the lighter Mg isotopic compositions of exchangeable Mg than that of the soil waters could be explained by ion-exchange processes. A basalt weathering profile indicated that the $\delta^{26}Mg$ values of the soils in the profile below 3 m are positively correlated with the abundance of kaolinite, while the opposite correlation was shown in the upper section (Huang et al., 2012). These authors explained that Mg adsorption onto soil surfaces initially favors heavy Mg isotopes, but the preferential desorption of heavy Mg isotopes through the ion exchange of Mg with relatively lower hydration energy ions (e.g., Sr^{2+} and Cs^{+}) could lead to the loss of heavy Mg isotopes from soils. In addition, a study that was conducted on the Madison aquifer suggested that the preferential uptake of light Mg isotopes during Mg-for-Na ion-exchange drives the water phases enriched in heavy Mg isotopes (Jacobson et al., 2010), implying that light Mg isotopes are retained in the solid phases. The typical similarity between these two case studies is that the solid phases are all long exposed to natural waters, i.e., soils in the upper section (<3 m) directly contacted rainwaters over a long time span (Huang et al., 2012) and dolomite was always exposed to surface water or groundwater (Jacobson et al., 2010). Given such favorable conditions, solid phases could easily interact with water phases under these conditions. During these interactions, Mg^{2+} ions from waters were taken up into solid phases and ion-exchange processes, i.e., desorption or Mg-for-Na exchange, may have occurred. Paddy soils are highly matured soils that have formed over much longer periods, which may provide sufficient time for soil minerals, such as kaolinite and Fe oxides, to interact with soil waters (Kögel-Knabner et al., 2010). Ion-exchange processes may thus cause heavier Mg isotopes to be preferentially released into water phases. Despite not knowing whether one or both of these ion-exchange processes occurred, we expect that light Mg isotopes were ultimately retained in exchangeable sites of minerals. This process can explain why exchangeable Mg had lighter Mg isotopic compositions than those of the soil waters.

5.3.2. Structural Mg

Unlike the exchangeable Mg, the structural Mg in the FMNs and surrounding soils exhibits distinguishable Mg isotopic compositions (Fig. 6), with an average $\Delta^{26}Mg_{FMN.stru\text{-}SS.stru}$ value of −0.94‰. Given the differently controlled minerals in these two parts, i.e., goethite in the FMNs and kaolinite in the surrounding soils, such distinct Mg isotopic compositions could be attributed to the different fractionation factors during its incorporation into the mineral structure. Assuming a constant isotope fractionation between the soil waters and the goethite, we could then define $\Delta^{26}Mg_{goethite\text{-}soil\ water}$ to be 0.31‰ based on the equation $\Delta^{26}Mg_{goethite\text{-}soil\ water} = \delta^{26}Mg_{goethite} - \delta^{26}Mg_{soil\ water}$. This value is comparable to the values in kaolinite-, gibbsite- and smectite-controlled soils (Teng et al., 2010; Huang et al., 2012; Liu et al., 2014), which showed $\Delta^{26}Mg_{soil\text{-}water}$ between 0.05 and 0.4‰. Therefore, the difference in fractionation factors could not be responsible

for the 0.94‰ difference in the isotopic compositions of structural Mg between the FMNs and surrounding soils. Alternatively, such a difference could be attributed to the different Mg sources in their structural sites. The surrounding soils are mainly derived from granite-weathering residues, so their structural Mg is mainly inherited from the parent granite. Although the isotope fractionation of Mg may occur during its incorporation into structural sites, heavy Mg isotopes are preferred in the crystal structure as suggested in previous studies (Wimpenny et al., 2014a). This is consistent with the heavy Mg isotopic compositions observed in the structural Mg of the surrounding soils (Fig. 6). However, unlike the surrounding soils, the FMNs are formed because of seasonally changing soil redox potential and pH (McKenzie, 1975; Palumbo et al., 2001; Liu et al., 2002; Tan et al., 2005, 2006; Jien et al., 2010; Yu et al., 2015). Under low redox potentials, Mg^{2+} ions can be released from Fe oxides; under high redox potentials, Mg^{2+} ions are again fixed into Fe oxides (Stoyanovsky and Cederbaum, 1998; Palumbo et al., 2001). This frequent release and incorporation of Mg^{2+} ions lead to the Mg from the soil waters fixed into the structure of Fe oxides. As discussed above, the soil waters are derived from carbonates and have significantly light Mg isotopic compositions. Therefore, the isotopic compositions of the structural Mg in the FMNs were heavier than those in the surrounding soils.

6. CONCLUSIONS AND IMPLICATIONS

This study presented the Mg isotopic compositions of FMNs, surrounding soils, exchangeable Mg, structural Mg, rocks, soil waters, rainwaters, stream waters, soil surface waters, and vegetation that developed on a paddy soil profile. In such hydromorphic soils, soluble Mg and exchangeable Mg in soil minerals directly controlled the Mg isotopic compositions in the soil system.

The distinct Mg isotopic compositions between the FMNs and surrounding soils reflected the different Mg sources in their crystal structure: the Mg in the FMNs was mainly derived from soil waters, while that in the surrounding soils was derived from the chemical weathering of the parent granite. Isotope fractionation occurred during the formation of Fe oxides because Mg^{2+} substitution for Fe^{3+} preferentially takes up heavier Mg isotopes. However, seasonally changing redox potential in soils could have caused Mg^{2+} ions from soil waters with light isotopes to become fixed into Fe oxides, creating bulk Fe oxides with light Mg isotopic compositions. The lighter Mg isotopic compositions in the surrounding soils could be explained by the retention of Mg^{2+} ions from soil waters in exchangeable sites of Mg-depleted clay minerals, such as kaolinite.

These findings are inconsistent with the most published reports, which stated that secondary clay minerals and metal oxides are enriched in heavy Mg isotopes (Fig. 10; Teng et al., 2010; Huang et al., 2012; Liu et al., 2014; Wimpenny et al., 2014a, 2014b). Our study provides field evidence that Mg-depleted clay minerals retain light Mg isotopes in their exchangeable sites and thus shift the Mg isotopic compositions of bulk soils towards lighter values.

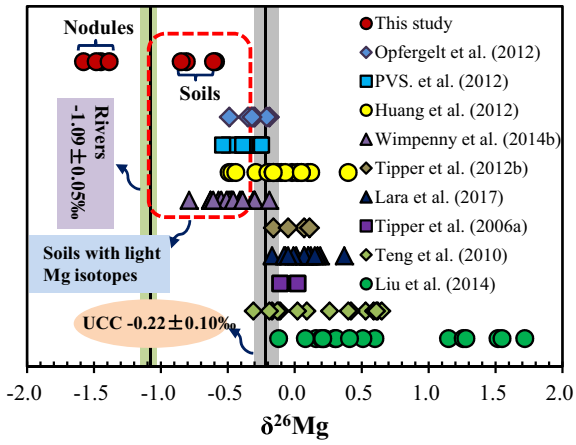

Fig. 10. Isotopic compositions of Mg in natural soils according to published literature and this study. The average $\delta^{26}Mg$ value of UCC from Li et al. (2010) and river waters from Tipper et al. (2006a) are plotted for reference.

Additionally, a new and important mechanism was demonstrated, in which Fe oxides in hydromorphic soils may drive the Mg isotopic compositions of soils towards lighter values. These findings are significant to explain why soils are sometimes enriched in lighter Mg isotopes relative to the parent rocks. This study highlights the roles of Mg-depleted clay minerals and Fe oxides in controlling the Mg isotopic compositions of soils.

ACKNOWLEDGMENTS

We thank Yuan Fang and Yahui Lv for their help when collecting samples. We also thank Yuhui Liu, Ruiying Li, Xu-Nan Meng, Yang Wang, Yue Peng, Hui Chang, and Dandan Li for their help in the clean room and MC-ICPMS lab. Yongsheng He, Jian-Ming Zhu, and Yiwen Lv are acknowledged for comments on the manuscript. This work was funded by the National Natural Science Foundation of China (41701266, U1612442, 41420104007, and 41561092), the Frontier Science Research Programme of the CAS (QYZDB-SSW-DQC046), the Science and Technology Foundation of Guangdong Province, China (2016B020242006 and 2016TX03Z086), the Scientific Platform and Innovation Capability Construction Program of the GDAS (2017GDASCX-0406 and 2017GDASCX-0106), and the One Hundred Talents Programme of the CAS.

REFERENCES

Ahrens L. H., Willis J. P. and Oosthuizen C. O. (1967) Further observations on the composition of manganese nodules, with particular reference to some of the rarer elements. *Geochim. Cosmochim. Acta* **31**, 2169–2180.

An Y., Wu F., Xiang Y., Nan X., Yu X., Yang J., Yu H., Xie L. and Huang F. (2014) High-precision Mg isotope analyses of low-Mg rocks by MC-ICP-MS. *Chem. Geol.* **390**, 9–21.

Appelo C. A. J. and Postma D. (2005) *Geochemistry, Groundwater and Pollution*, second ed. A.A Balkema.

Balistrieri L. S., Borrok D. M., Wanty R. B. and Ridley W. I. (2008) Fractionation of Cu and Zn isotopes during adsorption onto amorphous Fe (III) oxyhydroxide: experimental mixing of

acid rock drainage and ambient river water. *Geochim. Cosmochim. Acta* **72**, 311–328.

Baltpurvins K. A., Burns R. C., Lawrance G. A. and Stuart A. D. (1997) Effect of Ca^{2+}, Mg^{2+}, and anion type on the aging of iron (III) hydroxide precipitates. *Environ. Sci. Technol.* **31**, 1024–1032.

Bizzarro M., Paton C., Larsen K., Schiller M., Trinquier A. and Ulfbeck D. (2011) High-precision Mg-isotope measurements of terrestrial and extraterrestrial material by HR-MC-ICPMS—implications for the relative and absolute Mg-isotope composition of the bulk silicate Earth. *J. Anal. At. Spectrom.* **26**, 565–577.

Bolou-Bi E. B., Vigier N., Poszwa A., Boudot J. P. and Dambrine E. (2012) Effects of biogeochemical processes on magnesium isotope variations in a forested catchment in the Vosges Mountains (France). *Geochim. Cosmochim. Acta* **87**, 341–355.

Brenot A., Cloquet C., Vigier N., Carignan J. and France-Lanord C. (2008) Magnesium isotope systematics of the lithologically varied Moselle river basin. *France. Geochim. Cosmochim. Acta* **72**, 5070–5089.

Cabaret D., Sainctavit P., Ildefonse P. and Flank A. M. (1996) Full multiple-scattering calculations on silicates and oxides at the Al K edge. *J. Phys.-Condens. Mater.* **8**, 3691–3704.

Changela H. G., Bridges J. C. and Gurman S. J. (2012) Extended X-ray Absorption Fine Structure (EXAFS) in Stardust tracks: constraining the origin of ferric iron-bearing minerals. *Geochim. Cosmochim. Acta* **98**, 282–294.

Chapman H. D. (1965) *Cation Exchange Capacity: Methods of Soil Analysis*. American Society of Agronomy, Madison, pp. 891–901.

Chen H., Zhang W., Wang K. and Fu W. (2010) Soil moisture dynamics under different land uses on karst hillslope in northwest Guangxi, China. *Environ. Earth Sci.* **61**, 1105–1111.

Childs C. W. (1975) Composition of iron-manganese concretions from some New Zealand soils. *Geoderma* **13**, 141–152.

Cornell R. M. and Schwertmann U. (2003) *The Iron Oxides: Structure, Properties, Occurrences and Uses*. Wiley-VCH Verlag GmbH & Co., Weinheim, pp. 1–664.

Drever J. I. (1988) *The Geochemistry of Natural Waters*. Prentice Hall, New Jersey.

Foster G. L., Pogge von Strandmann P. A. and Rae J. W. B. (2010) Boron and magnesium isotopic composition of seawater. *Geochem. Geophys. Geosyst.* **11**.

Galy A., Bar-Matthews M., Halicz L. and O'Nions R. K. (2002) Mg isotopic composition of carbonate: insight from speleothem formation. *Earth Planet. Sci. Lett.* **201**, 105–115.

Galy A., Yoffe O., Janney P. E., Williams R. W., Cloquet C., Alard O. and Carignan J. (2003) Magnesium isotope heterogeneity of the isotopic standard SRM980 and new reference materials for magnesium-isotope-ratio measurements. *J. Anal. At. Spectrom.* **18**, 1352–1356.

Gao T., Ke S., Teng F.-Z., Chen S., He Y. S. and Li S.-G. (2016) Magnesium isotope fractionation during dolostone weathering. *Chem. Geol.* **445**, 14–23.

Gasparatos D. (2012) Fe-Mn concretions and nodules to sequester heavy metals in soils. *Environ. Chem Sustain. World* **Part 2**, 443–472.

He Z., Zhang M. and Wilson M. J. (2004) Distribution and classification of red soils in China. *Red Soils China*, 29–33.

Huang K.-J., Teng F.-Z., Wei G.-J., Ma J.-L. and Bao Z.-Y. (2012) Adsorption-and desorption-controlled magnesium isotope fractionation during extreme weathering of basalt in Hainan Island, China. *Earth Planet. Sci. Lett.* **359**, 73–83.

Huang K.-J., Teng F.-Z., Elsenouy A., Li W.-Y. and Bao Z.-Y. (2013) Magnesium isotopic variations in loess: origins and implications. *Earth Planet. Sci. Lett.* **374**, 60–70.

Jacobson A. D., Zhang Z., Lundstrom C. and Huang F. (2010) Behavior of Mg isotopes during dedolomitization in the Madison Aquifer, South Dakota. *Earth Planet. Sci. Lett.* **297**, 446–452.

Jien S. H., Hseu Z. Y. and Chen Z. S. (2010) Hydropedological implications of ferromanganiferous nodules in rice-growing plinthitic Ultisols under different moisture regimes. *Soil Sci. Soc. Am. J.* **74**, 880–891.

Jolsterå R., Gunneriusson L. and Holmgren A. (2012) Surface complexation modeling of Fe_3O_4–H^+ and Mg (II) sorption onto maghemite and magnetite. *J. Colloid Interf. Sci.* **386**, 260–267.

Juillot F., Maréchal C., Ponthieu M., Cacaly S., Morin G., Benedetti M., Hazemann J. L., Proux O. and Guyot F. (2008) Zn isotopic fractionation caused by sorption on goethite and 2-Lines ferrihydrite. *Geochim. Cosmochim. Acta* **72**, 4886–4900.

Ke S., Teng F.-Z., Li S.-G., Gao T., Liu S.-A., He Y. and Mo X. (2016) Mg, Sr, and O isotope geochemistry of syenites from northwest Xinjiang, China: tracing carbonate recycling during Tethyan oceanic subduction. *Chem. Geol.* **437**, 109–119.

Kim Y., Cygan R. T. and Kirkpatrick R. J. (1996) ^{133}Cs NMR and XPS investigation of cesium adsorbed on clay minerals and related phases. *Geochim. Cosmochim. Acta* **60**, 1041–1052.

Kinniburgh D. G., Jackson M. L. and Syers J. K. (1976) Adsorption of alkaline earth, transition, and heavy metal cations by hydrous oxide gels of iron and aluminum. *Soil Sci. Soc. Am. J.* **40**, 796–799.

Kögel-Knabner I., Amelung W., Cao Z., Fiedler S., Frenzel P., Jahn R., Kalbitz K., Kölbl A. and Schloter M. (2010) Biogeochemistry of paddy soils. *Geoderma* **157**, 1–14.

Kosmulski M. (2006) pH-dependent surface charging and points of zero charge: III Update. *J. Colloid Interf. Sci.* **298**, 730–741.

Ladeira A. C. Q., Ciminelli V. S. T., Duarte H. A., Alves M. C. M. and Ramos A. Y. (2001) Mechanism of anion retention from EXAFS and density functional calculations: Arsenic (V) adsorbed on gibbsite. *Geochim. Cosmochim. Acta* **65**, 1211–1217.

Lara M. C., Buss H. L., von Strandmann P. A. P., Schuessler J. A. and Moore O. W. (2017) The influence of critical zone processes on the Mg isotope budget in a tropical, highly weathered andesitic catchment. *Geochim. Cosmochim. Acta* **202**, 77–100.

Li W., Beard B. L. and Johnson C. M. (2011) Exchange and fractionation of Mg isotopes between epsomite and saturated $MgSO_4$ solution. *Geochim. Cosmochim. Acta* **75**, 1814–1828.

Li W., Chakraborty S., Beard B. L., Romanek C. S. and Johnson C. M. (2012) Magnesium isotope fractionation during precipitationof inorganic calcite under laboratory conditions. *Earth Planet. Sci. Lett.* **333**, 304–316.

Li W., Beard B. L., Li C. and Johnson C. M. (2014) Magnesium isotope fractionation between brucite [$Mg(OH)_2$] and Mg aqueous species: implications for silicate weathering and biogeochemical processes. *Earth Planet. Sci. Lett.* **394**, 82–93.

Li W., Beard B. L., Li C., Xu H. and Johnson C. M. (2015) Experimental calibration of Mg isotope fractionation between dolomite and aqueous solution and its geological implications. *Geochim. Cosmochim. Acta* **157**, 164–181.

Li W.-Y., Teng F.-Z., Ke S., Rudnick R. L., Gao S., Wu F.-Y. and Chappell B. W. (2010) Heterogeneous magnesium isotopic composition of the upper continental crust. *Geochim. Cosmochim. Acta* **74**, 6867–6884.

Ling M. X., Sedaghatpour F., Teng F.-Z., Hays P. D., Strauss J. and Sun W. (2011) Homogeneous magnesium isotopic composition of seawater: an excellent geostandard for Mg isotope analysis. *Rapid Commun. Mass Spectrom.* **25**, 2828–2836.

Liu F., Colombo C., Adamo P., He J. Z. and Violante A. (2002) Trace elements in manganese-iron nodules from a Chinese Alfisol. *Soil Sci. Soc. Am. J.* **66**, 661–670.

Liu X.-M., Teng F.-Z., Rudnick R. L., McDonough W. F. and Cummings M. L. (2014) Massive magnesium depletion and isotope fractionation in weathered basalts. *Geochim. Cosmochim. Acta* **135**, 336–349.

Ma H., Xu Y., Huang K., Sun Y., Ke S., Peng Y., Lang X., Yan Z. and Shen B. (2018) Heterogeneous Mg isotopic composition of the early Carboniferous limestone: implications for carbonate as a seawater archive. *Acta Geochim.* **37**, 1–18.

Ma L., Teng F.-Z., Jin L., Ke S., Yang W., Gu H. O. and Brantley S. L. (2015) Magnesium isotope fractionation during shale weathering in the Shale Hills Critical Zone Observatory: accumulation of light Mg isotopes in soils by clay mineral transformation. *Chem. Geol.* **397**, 37–50.

McKenzie R. M. (1975) An electron microprobe study of the relationships between heavy metals and manganese and iron in soils and ocean floor nodules. *Soil Res.* **13**, 177–188.

Merkel B. and Planer-Friedrich B. (2008) *Groundwater Geochemistry: A Practical Guide to Modeling of Natural and Contaminated Aquatic Systems*. Springer Verlag.

Montezano A. C., Antunes T. T., Callera G. and Touyz R. M. (2013) Magnesium and vessels. In *Encyclopedia of Metalloproteins*. Springer, New York, pp. 1238–1243.

Odom I. (1984) Smectite clay minerals: properties and uses. *Philos. Trans. R. Soc. Lond. Ser. A Math. Phys. Sci.* **311**, 391–409.

Opfergelt S., Georg R. B., Delvaux B., Cabidoche Y. M., Burton K. W. and Halliday A. N. (2012) Mechanisms of magnesium isotope fractionation in volcanic soil weathering sequences, Guadeloupe. *Earth Planet. Sci. Lett.* **341**, 176–185.

Opfergelt S., Burton K. W., Georg R. B., West A. J., Guicharnaud R. A., Sigfusson B. and Halliday A. N. (2014) Magnesium retention on the soil exchange complex controlling Mg isotope variations in soils, soil solutions and vegetation in volcanic soils, Iceland. *Geochim. Cosmochim. Acta* **125**, 110–130.

Paikaray S., Essilfie-Dughan J. and Hendry M. J. (2018) Ionic substitution of Mg^{2+} for Al^{3+} and Fe^{3+} with octahedral coordination in hydroxides facilitate precipitation of layered double hydroxides. *Geochim. Cosmochim. Acta* **220**, 217–234.

Palumbo B., Bellanca A., Neri R. and Roe M. J. (2001) Trace metal partitioning in Fe–Mn nodules from Sicilian soils, Italy. *Chem. Geol.* **173**, 257–269.

Pavlov M., Siegbahn P. E. and Sandström M. (1998) Hydration of beryllium, magnesium, calcium, and zinc ions using density functional theory. *J. Phys. Chem. A* **102**, 219–228.

Pogge von Strandmann P. A., Burton K. W., James R. H., van Calsteren P., Gislason S. R. and Sigfússon B. (2008a) The influence of weathering processes on riverine magnesium isotopes in a basaltic terrain. *Earth Planet. Sci. Lett.* **276**, 187–197.

Pogge von Strandmann P. A., James R. H., van Calsteren P., Gíslason S. R. and Burton K. W. (2008b) Lithium, magnesium and uranium isotope behaviour in the estuarine environment of basaltic islands. *Earth Planet. Sci. Lett.* **274**, 462–471.

Pogge von Strandmann P. A., Opfergelt S., Lai Y. J., Sigfússon B., Gislason S. R. and Burton K. W. (2012) Lithium, magnesium and silicon isotope behaviour accompanying weathering in a basaltic soil and pore water profile in Iceland. *Earth Planet. Sci. Lett.* **339**, 11–23.

Pokrovsky O. S., Viers J. and Freydier R. (2005) Zinc stable isotope fractionation during its adsorption on oxides and hydroxides. *J. Colloid Interf. Sci.* **291**, 192–200.

Pokrovsky O. S., Viers J., Emnova E. E., Kompantseva E. I. and Freydier R. (2008) Copper isotope fractionation during its interaction with soil and aquatic microorganisms and metal oxy (hydr)oxides: possible structural control. *Geochim. Cosmochim. Acta* **72**, 1742–1757.

Ryu J. S., Jacobson A. D., Holmden C., Lundstrom C. and Zhang Z. (2011) The major ion, $\delta^{44/40}$Ca, $\delta^{44/42}$Ca, and $\delta^{26/24}$Mg geochemistry of granite weathering at pH = 1 and T = 25°C: power-law processes and the relative reactivity of minerals. *Geochim. Cosmochim. Acta* **75**, 6004–6026.

Ryu J. S., Vigier N., Decarreau A., Lee S. W., Lee K. S., Song H. and Petit S. (2016) Experimental investigation of Mg isotope fractionation during mineral dissolution and clay formation. *Chem. Geol.* **445**, 135–145.

Saenger C. and Wang Z. (2014) Magnesium isotope fractionation in biogenic and abiogenic carbonates: implications for paleoenvironmental proxies. *Quat. Sci. Rev.* **90**, 1–21.

Schauble E. A. (2004) Applying stable isotope fractionation theory to new systems. *Rev. Mineral. Geochem.* **55**, 65–111.

Schmitt A. D., Vigier N., Lemarchand D., Millot R., Stille P. and Chabaux F. (2012) Processes controlling the stable isotope compositions of Li, B, Mg and Ca in plants, soils and waters: a review. *CR Geosci.* **344**, 704–722.

Scroth B. K. and Sposito G. (1997) Surface charge properties of kaolinite. *Clays Clay Miner.* **45**, 85–91.

Shannon R. D. T. and Prewitt C. T. (1969) Effective ionic radii in oxides and fluorides. *Acta Crystall. Sect. B: Struct. Crystall. Cryst. Chem.* **25**, 925–946.

Sposito G. (1989) *The Chemistry of Soil*. Oxford Univ. Press, New York.

Stoyanovsky D. A. and Cederbaum A. I. (1998) Redox-cycling of iron ions triggers calcium release from liver microsomes. *Free Radical Bio. Med.* **24**, 745–753.

Tan W.-F., Liu F., Feng X. H., Huang Q. Y. and Li X. Y. (2005) Adsorption and redox reactions of heavy metals on FMNs from Chinese soils. *J. Colloid Interf. Sci.* **284**, 600–605.

Tan W.-F., Liu F., Li Y.-H., Hu H.-Q. and Huang Q. Y. (2006) Elemental composition and geochemical characteristics of iron-manganese nodules in main soils of China. *Pedosphere* **16**, 72–81.

Teng F.-Z., Li W.-Y., Rudnick R. L. and Gardner L. R. (2010) Contrasting lithium and magnesium isotope fractionation during continental weathering. *Earth Planet. Sci. Lett.* **300**, 63–71.

Teng F.-Z., Li W.-Y., Ke S., Yang W., Liu S.-A., Sedaghatpour F., Wang S.-J., Huang K.-J., Hu Y., Ling M.-X., Xiao Y., Liu X.-M., Li X.-W., Gu H.-O., Sio C. K., Wallace D. A., Su B.-X., Zhao L., Chamberlin J., Harrington M. and Brewer A. (2015) Magnesium isotopic compositions of international geological reference materials. *Geostand. Geoanal. Res.* **39**, 329–339.

Teng F.-Z. (2017) Magnesium isotope geochemistry. *Rev. Mineral. Geochem.* **82**, 219–287.

Tessier A., Campbell P. G. and Bisson M. (1979) Sequential extraction procedure for the speciation of particulate trace metals. *Anal. Chem.* **51**, 844–851.

Tipper E. T., Galy A. and Bickle M. J. (2006a) Riverine evidence for a fractionated reservoir of Ca and Mg on the continents: implications for the oceanic Ca cycle. *Earth Planet. Sci. Lett.* **247**, 267–279.

Tipper E. T., Galy A., Gaillardet J., Bickle M. J., Elderfield H. and Carder E. A. (2006b) The magnesium isotope budget of the modern ocean: constraints from riverine magnesium isotope ratios. *Earth Planet. Sci. Lett.* **250**, 241–253.

Tipper E. T., Gaillardet J., Louvat P., Capmas F. and White A. F. (2010) Mg isotope constraints on soil pore-fluid chemistry: evidence from Santa Cruz. *California. Geochim. Cosmochim. Acta* **74**, 3883–3896.

Tipper E. T., Calmels D., Gaillardet J., Louvat P., Capmas F. and Dubacq B. (2012a) Positive correlation between Li and Mg

isotope ratios in the river waters of the Mackenzie Basin challenges the interpretation of apparent isotopic fractionation during weathering. *Earth Planet. Sci. Lett.* **333**, 35–45.

Tipper E. T., Lemarchand E., Hindshaw R. S., Reynolds B. C. and Bourdon B. (2012b) Seasonal sensitivity of weathering processes: Hints from magnesium isotopes in a glacial stream. *Chem. Geol.* **312**, 80–92.

Urey H. C. (1947) The thermodynamic properties of isotopic substances. *J. Chem. Soc.*, 562–581.

Wang S.-J., Teng F.-Z., Rudnick R. L. and Li S.-G. (2015) The behavior of magnesium isotopes in low-grade metamorphosed mudrocks. *Geochim. Cosmochim. Acta* **165**, 435–448.

Wang S.-J. and Wasylenki L. E. (2017) Experimental constraints on reconstruction of Archean seawater Ni isotopic composition from banded iron formations. *Geochim. Cosmochim. Acta* **206**, 137–150.

Wilkinson S., Welch R., Mayland H. and Grunes D. (1990) Magnesium in plants: uptake, distribution, function and utilization by man and animals. *Met. Ions Biol. Syst.* **26**, 33–56.

Wimpenny J., Gíslason S. R., James R. H., Gannoun A., Von Strandmann P. A. P. and Burton K. W. (2010) The behaviour of Li and Mg isotopes during primary phase dissolution and secondary mineral formation in basalt. *Geochim. Cosmochim. Acta* **74**, 5259–5279.

Wimpenny J., Colla C. A., Yin Q.-Z., Rustad J. R. and Casey W. H. (2014a) Investigating the behaviour of Mg isotopes during the formation of clay minerals. *Geochim. Cosmochim. Acta* **128**, 178–194.

Wimpenny J., Yin Q. Z., Tollstrup D., Xie L. W. and Sun J. (2014b) Using Mg isotope ratios to trace Cenozoic weathering changes: A case study from the Chinese Loess Plateau. *Chem. Geol.* **376**, 31–43.

Young E. D. and Galy A. (2004) The isotope geochemistry and cosmochemistry of magnesium. *Rev. Mineral. Geochem.* **55**, 197–230.

Yu X., Fu Y., Brookes P. C. and Lu S. G. (2015) Insights into the Formation process and environmental fingerprints of iron-manganese nodules in subtropical soils of China. *Soil Sci. Soc. Am.* **79**, 1101–1111.

Associate editor: Andrew D. Jacobson